

Critical comparison of OII(732–733 nm), OI(630 nm), and N₂(1PG) emissions in auroral rays

Joshua Semeter

SRI International, Menlo Park, CA, USA

Received 6 July 2002; revised 3 September 2002; accepted 13 September 2002; published 11 March 2003.

[1] All-sky spectral imagery has been used to study the altitude distribution of OII(732–733 nm), OI(630 nm), and N₂(1PG) emissions in tall auroral rays appearing at the poleward edge of the auroral oval. The OII(732–733 nm) emission layer was consistently higher than the OI(630 nm) emission layer in these structures; the peak emission altitudes were estimated to be ~380 km and ~240 km, respectively. Neither the high absolute altitude of the OII(732–733 nm) peak nor its >100 km offset from the OI(630 nm) peak are consistent with published model results, which consider electron impact on atomic oxygen as the sole source of auroral O⁺(²P). The present results suggest that O⁺(²P) may also be excited directly from ambient ionospheric O⁺(⁴S) atoms. Other contributing factors may include a significant underestimation of the rate coefficients for O⁺(²P) quenching, or field-aligned up-flows of ionospheric O⁺. **INDEX TERMS:** 2407 Ionosphere: Auroral ionosphere (2704); 2455 Particle precipitation; 2736 Magnetospheric Physics: Magnetosphere/ionosphere interactions; 2716 Energetic particles, precipitating. **Citation:** Semeter, J., Critical comparison of OII(732–733 nm), OI(630 nm), and N₂(1PG) emissions in auroral rays, *Geophys. Res. Lett.*, 30(5), 1225, doi:10.1029/2002GL015828, 2003.

1. Introduction

[2] Despite the proliferation of monochromatic imaging systems in the auroral zone, reported results have been limited almost exclusively to three spectral features: the O(¹D–³P) transition at 630 nm, the N₂⁺ first negative system (1NG) sampled at 427.8 nm, and the O(¹S–³P) transition at 557.7 nm. The high intensity and spectral purity of these emissions have facilitated their extensive use in studies of auroral energetics and atmospheric composition. Other emissions could yield equal or greater insight in an imaging context, but require a more sophisticated analysis to be resolved.

[3] One such emission is the OII(732–733 nm) doublet, produced by the O⁺(²P–⁴S) transition. The excited O⁺(²P) configuration is produced directly from soft electron impact (<100 eV) on neutral atomic oxygen [Omholt, 1957; Sivjee et al., 1979; Rees et al., 1982]. The diagnostic value of OII(732–733 nm) lies in its relationship to F-region ionization by auroral precipitation. Unfortunately, the emission has neither of the observational advantages mentioned above: its integrated intensity is less than 300 Rayleighs [Lummerzheim et al., 1990], and it is superposed on the

(5,3) emission band of the N₂ first positive group (1PG) (see Sivjee et al. [1999] for representative spectra).

[4] Imaging OII(732–733 nm) requires a means of removing the N₂(1PG) sources at 732–733 nm. Semeter et al. [2001] treated this problem using images of N₂⁺(427.8 nm) as a proxy for the N₂(1PG) contribution in the 732–733 nm band. Through this multispectral approach, they showed that the OII(732–733 nm) source can dominate the 732–733 nm band even in narrow (<1 km) auroral arcs during periods of arc formation.

[5] In this work, we resolve images of OII(732–733 nm) in another way - namely, by exploiting differences in emission altitude between the competing O⁺(²P) and N₂(1PG) sources revealed when auroral rays are viewed obliquely to the field line. In comparing such images to the same auroral forms imaged at 630 nm, we found that the OII(732–733 nm) emission peak appeared consistently above the OI(630 nm) peak. This result is inconsistent with published theoretical predictions; possible mechanisms and consequences are discussed.

2. Experiment

[6] On the night of 20–21 November 2001, a combined radar-optical experiment was conducted at Sondrestrom, Greenland, to study the ionospheric response to auroral precipitation at high spatial and temporal resolution. The Sondrestrom all-sky imager (ASI) was operated using the three-filter sequence summarized in Table 1. Channel 2 captures the 630 nm redline emission of atomic oxygen, and the remaining two channels provide the unique combination needed to isolate the OII(732–733 nm) doublet. Channel 1 images wavelengths longer than 645 nm. In this regime (specifically, from 640 to 800 nm) the auroral spectrum is dominated by the intense band structure of N₂(1PG) (e.g., Figures 5.17 and 5.18 of Chamberlain [1961]). In fact, the integrated intensity of these bands is expected to always dominate the other features in this interval, such that an image of the discrete aurora through Channel 1 can be considered a spectrally pure representation of N₂(1PG). Channel 3 images a 3 nm band within the pass band of Channel 1. Because of its narrow bandwidth, the OII(732–733 nm) and N₂(1PG) sources have comparable intensities in Channel 3, but the N₂(1PG) component will be proportional to Channel 1. This suggests that Channels 1 and 3 could be combined to yield a spectrally pure image of OII(732–733 nm). This logic forms the basis of our analysis.

3. Results

[7] From 0130–0500 UT on 21 November 21 2001, the aurora was characterized by tall, rayed, arcs stretching to the

Table 1. Salient Filter Characteristics

| Channel | Filter Band (nm) | Exposure (s) | Spectral Feature |
|---------|------------------|--------------|---------------------------------------|
| 1 | >645 | 0.5 | N ₂ (1PG) |
| 2 | 629.8–630.8 | 0.5 | OI(630 nm) |
| 3 | 731.5–733.5 | 20.0 | OII(732–733 nm), N ₂ (1PG) |

magnetic east and west horizons. The arcs generally formed to the magnetic north, then propagated southward and faded. In many instances, the arcs appeared initially as individual rays, persisting as stable structures for 10's of seconds before brightening and propagating southward. Since our analysis requires targets to remain stationary for 21 s, it is these stable rays that are of primary interest.

[8] Figure 1 presents five multispectral image sequences of stable rayed aurora recorded during a half-hour period of clear skies near local midnight. The full 180° field of view is shown, with north toward the bottom and west toward the left. The magnetic zenith is indicated by the white box and the universal time at the start of the exposure is shown in the lower left. The first two rows are contiguous to illustrate the time stationarity of the observed structures.

[9] Using the top row as an example, Channel 1 (0302:16 UT) shows a rayed arc along the northern horizon. In Channel 2 (0302:18 UT), the same arc appears closer to the zenith and more diffuse. This is expected since OI(630 nm) occurs at a higher altitude and has a long (~110 s) radiative lifetime. In Channel 3 (0302:21 UT) the arc is seen to have two maxima: the fainter band near the horizon is caused by the N₂(1PG) source - the source imaged in Channel 1 - and the higher elevation band is produced by OII(732–733 nm).

[10] To assist in interpreting these measurements, the right-hand column gives composite images constructed by assigning a unique color to each channel: blue to Channel 1, red to Channel 2, and green to Channel 3. Note that the colors are organized along lines that converge precisely in the magnetic zenith. This is a clear indication that we are seeing an organization of emission sources along magnetic field lines rather than across them. Note also that the red color (630 nm) appears between the two sources imaged in Channel 3 and above the source imaged by Channel 1. This effect can be seen in all examples shown, and is the critical observation of this work.

4. Analysis of Emission Profiles

[11] A simple geometric analysis based on reasonable assumptions was applied to place some limits on the observed altitude separation. First, photometric and geometric calibrations were carried out such that curves of brightness versus elevation angle could be extracted. Figure 2a gives the brightness extracted along the line bracketed by the two arrows in the lower-right image of Figure 1. The color coding from Figure 1 has been retained. The red curve (Channel 2) corresponds to the left ordinate and the green curve (Channel 3) to the right ordinate; the blue curve (Channel 1) has been normalized to the lower peak of the green curve. Recall that the lower peak of Channel 3 is produced by the same N₂(1PG) source as Channel 1. Their precise co-alignment in elevation angle provides additional strong evidence that the auroral flux tube did not move appreciably during the acquisition period.

[12] Second, we subtracted the background contribution in each channel. The auroral structures in Figure 1 were, in fact, embedded in a bright diffuse background; in Figure 2, for instance, the redline brightness in the magnetic zenith was nearly 2 kR. That this background was caused by a diffuse auroral source was confirmed by incoherent scatter (IS) radar elevation scans, which measured a uniform E-region density of $\sim 5 \times 10^{11} \text{m}^{-3}$ from horizon to horizon during this period. For our initial analysis, we modeled the background as a uniform emitting layer. With respect to Figure 2a, this amounted to subtracting the path-length corrected brightness that makes the brightness go to 0 at 90° elevation, where no visible arcs were present.

[13] Next, we converted elevation angle to altitude by applying the geometric model shown in Figure 2b. The arc was assumed to be thin in the direction perpendicular to the line of sight. Here, D is the local magnetic dip angle, θ the elevation angle, ϵ the brightness, and z altitude (a flat-Earth approximation was used). The auroral flux tube is defined in a physical coordinate system by specifying the elevation θ_1 and altitude z_1 of a single point along the auroral ray. Figure 2b shows the altitude emission curves that result from fixing the N₂(1PG) emission peak at an altitude of 110 km. While somewhat arbitrary, this value is consistent with modeled N₂⁺(1NG) emission profiles for ~1 keV electrons [Strickland *et al.*, 1989]. The parameter plotted in Figure 2c is ϵ_{\perp} in Figure 2b - the surface brightness normal to the flux tube.

[14] This choice for z_1 resulted in an OI(630 nm) emission peak of ~240 km - also consistent with various theoretical calculations [e.g. Meier *et al.*, 1989; Solomon *et al.*, 1988] - and an OII(732–733 nm) peak of ~380 km. Choosing a lower altitude for the N₂(1PG) emission peak will decrease the estimated separation between the OI(630 nm) and OII(732–733 nm) peaks. But even at an extreme lower value of $z_1 = 90$ km, the separation is 100 km. For $z_1 = 170$ km the separation grows to 200 km.

[15] Finally, we derived an estimate of the spectrally pure OII(732–733 nm) profile by subtracting the normalized Channel 1 profile from the Channel 3 profile (i.e., green minus blue). Figure 2d compares the resultant OII(732–733 nm) and OI(630 nm) emission curves on a logarithmic scale.

5. Discussion

[16] The altitude separation among the OII(732–733 nm), OI(630 nm), and N₂(1PG) emissions, dramatically imaged in Figure 1, was evident in all image sequences analyzed on this evening, regardless of the location of the aurora, and regardless of whether the aurora was approaching or retreating from the zenith. The separation between the N₂(1PG) and OI(630 nm) peaks was expected, but the few published model results concerning auroral OII(732–733 nm) emission altitudes predict a close alignment with OI(630 nm) peak [Rees and Jones, 1973; Torr and Torr, 1982; Semeter *et al.*, 2001].

[17] Although O⁺(²P) and O(¹D) are both produced by electron impact on neutral atomic oxygen, O⁺(²P) requires 18.61 eV, compared with 1.96 eV for O(¹D). For this reason, chemical reactions, in particular dissociative recombination with O₂⁺, remain the dominant source of auroral O(¹D) [Meier *et al.*, 1989]. However, it is problematic to try

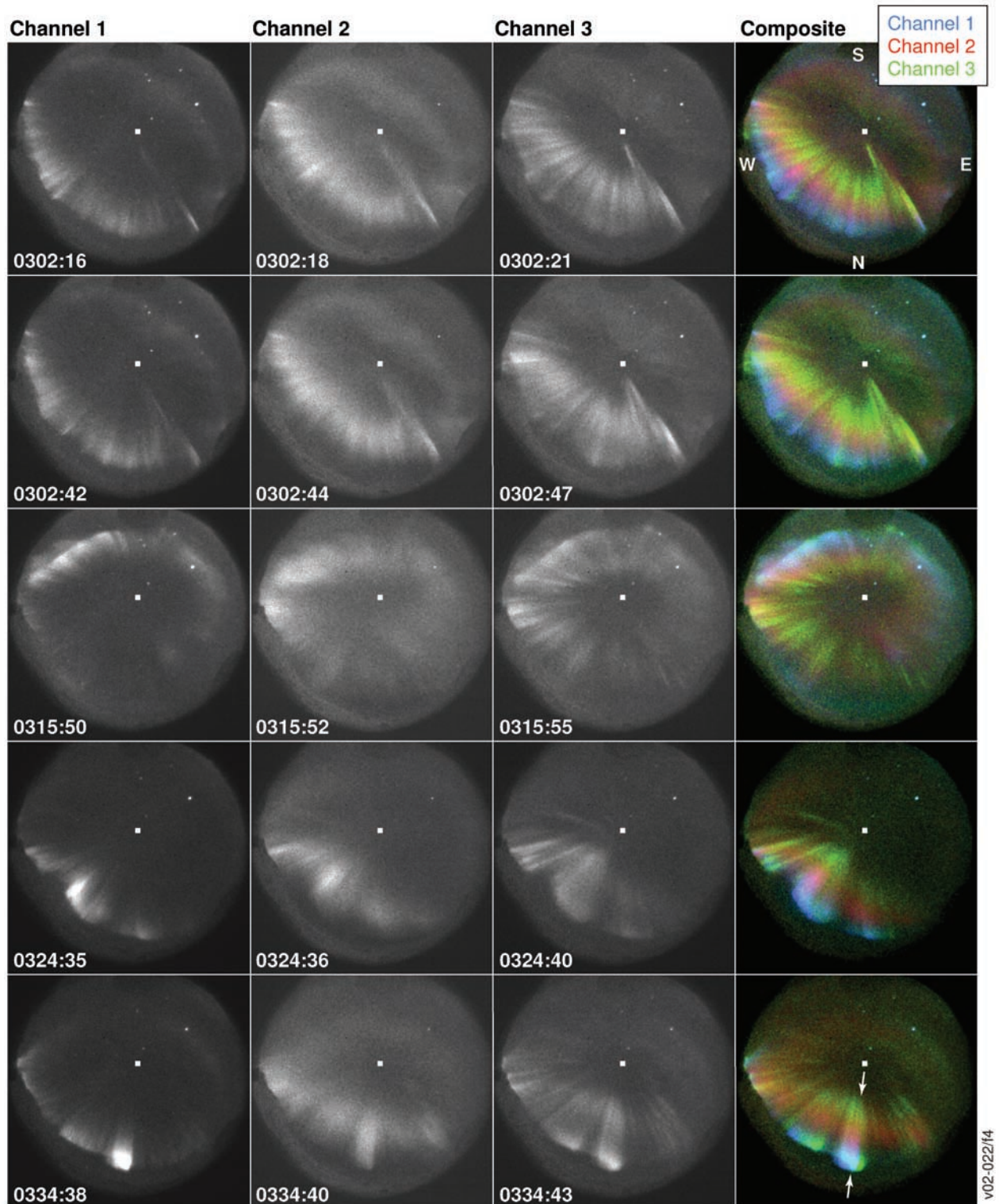


Figure 1. Multispectral all-sky image sequences (left three columns) and associated composite color images (right column) of rayed aurora on the evening of 20 November, 2002. Note the distinct organization of the colors along magnetic field lines.

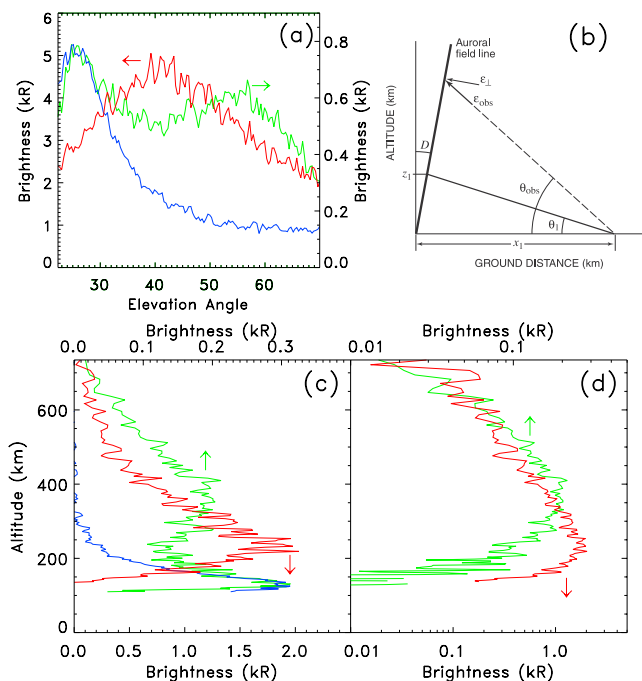


Figure 2. (a) Brightness versus elevation angle along the flux tube indicated by the arrows in Figure 1, lower right. (b) Geometry used to extract altitude emission profiles. (c) Brightness versus altitude, resolved using the geometric model of Figure 2b. (d) The pure OII (732–733 nm) profile after subtraction of N₂ (1PG) contribution, compared with OI (630 nm).

to account for the observed discrepancy through such additional sources. If one considers only the electron impact source for both emissions, the resulting OII(732–733 nm) and OI(630 nm) emission profiles will be nearly proportional since $O^+(^2P)$ and $O(^1D)$ are both excited from the isotropic secondary electron population. Current models predict that all additional sources of auroral OI(630 nm) peak at higher altitudes than the electron impact source, hence raising the OI(630 nm) emission peak with respect to the OII(732–733 nm) peak. The mechanism we require must have exactly the opposite effect.

[18] The cause of the observed altitude separation thus remains unclear. The extreme altitude separation is suggestive of an additional source for auroral $O^+(^2P)$, perhaps via direct excitation of ambient $O^+(^4S)$ atoms. Another contributing factor could be a significant underestimation of the currently accepted rate coefficients for $O^+(^2P)$ quenching via O and N_2 . Increased quenching would decrease preferentially lower altitude $O^+(^2P)$ thus raising the expected emission peak. The model results reported by Semeter *et al.* [2001], for example, used the quenching rates of Rusch *et al.* [1977], which were found by Bucselo *et al.* [1998] to provide a better fit to their 247 nm measurements than the higher Chang *et al.* [1993] results. Still another contributing mechanism could be vertical transport of O^+ . Such ion upflows are commonly observed by IS radars at auroral latitudes [Ogawa *et al.*, 2000] and by polar orbiting satellites at the polar cap boundary [McFadden *et al.*, 2001].

Because of the 5 s radiative lifetime of the forbidden OII(732–733 nm) emission, vertical transport would cause the emission to be “smeared” upward along the field line. The distinct separation of the OII(732–733 nm) and OI(630 nm) emission peaks seen in Figure 2, however, could not be produced by this mechanism.

6. Summary

[19] The contribution of this work is twofold. First, we have described a technique for isolating the OII(732–733 nm) doublet in auroral imagery by means of its altitude separation from the competing N₂(1PG) source in the 732–773 nm band. Second, we have used this technique to discover a significant altitude separation between the OII(732–733 nm) and OI(630 nm) emission peaks in a series of tall auroral rays observed near the polar cap boundary. The >100 km offset between the emission peaks is inconsistent with published predictions; further modeling is required to understand this result.

[20] **Acknowledgments.** The author thanks Jeffrey Thayer, Dirk Lummerzheim, and Richard Doe for valuable discussions, and the Sondrestrom site crew for support during the November 2001 campaign. This work was partially supported by NSF grant ATM-9813556.

References

- Bucselo, E., et al., Atomic and molecular emissions in the middle ultraviolet dayglow, *J. Geophys. Res.*, 103, 29,215–29,228, 1998.
- Chamberlain, J., *Physics of the Aurora and Airglow*, Academic, New York, 1961.
- Chang, T., et al., Reevaluation of the $O^+(^2P)$ reaction rate coefficients derived from Atmosphere Explorer C observations, *J. Geophys. Res.*, 98, 15,589–15,597, 1993.
- Lummerzheim, D., et al., The application of spectroscopic studies of the aurora thermospheric neutral composition, *Planet. Space Sci.*, 38, 67–78, 1990.
- McFadden, J., et al., FAST observations of ion outflow associated with magnetic storms, *Space Weather: Geophysical Monograph*, 125, 413, 2001.
- Meier, R., et al., Deducing composition and incident electron spectra from ground-based auroral optical measurements: A study of auroral red line processes, *J. Geophys. Res.*, 94, 13,541–13,552, 1989.
- Ogawa, Y., et al., Simultaneous EISCAT Svalbard and VHF radar observations of ion upflow at different aspect angles, *GRL*, 27, 81–84, 2000.
- Omholt, A., The red and near-infrared auroral spectrum, *J. Atmos. Terr. Phys.*, 10, 320–331, 1957.
- Rees, M., et al., The production efficiency of $O^+(^2P)$ ions by auroral electron impact ionization, *J. Geophys. Res.*, 87, 3612–3616, 1982.
- Rees, M. H., and R. Jones, Time-dependent studies of the aurora-II. Spectroscopic morphology, *Planet. Space Sci.*, 21, 1213–1235, 1973.
- Rusch, D., et al., The OII(7319–7330 Å) dayglow, *J. Geophys. Res.*, 82, 719–722, 1977.
- Semeter, J., et al., Simultaneous multispectral imaging of the discrete aurora, *J. Atmos. Sol. Terr. Phys.*, 63, 1981–1992, 2001.
- Sivjee, G., et al., Intensity ratio and center wavelengths of OII (7320–7330 Å) line emissions, *The Astrophysical Journal*, 229, 432–438, 1979.
- Sivjee, G., et al., Variations, with peak emission altitude, in auroral O₂ atmospheric (1,1)/(0,1) ratios and its relation to other auroral emissions, *J. Geophys. Res.*, 104, 28,003–28,018, 1999.
- Solomon, S., et al., The auroral 6300 Å emission: Observations and modeling, *J. Geophys. Res.*, 93, 9867–9882, 1988.
- Strickland, D., et al., Deducing composition and incident electron spectra from ground-based auroral optical measurements: Theory and results, *J. Geophys. Res.*, 94, 13,527–13,539, 1989.
- Torr, M., and D. Torr, The role of metastable species in the thermosphere, *Rev. Geophys.*, 20, 91–144, 1982.